

Transfer of a Tetramethylammonium Ion across the Water–Nitrobenzene Interface: Potential of Mean Force and Nonequilibrium Dynamics

Karl Schweighofer and Ian Benjamin*

Department of Chemistry, University of California Santa Cruz, California 95064

Received: June 15, 1999; In Final Form: August 3, 1999

The transfer of a tetramethylammonium ion across the water/nitrobenzene liquid/liquid interface is studied at 300 K using molecular dynamics computer simulations. The potential of mean force, calculated using two different techniques, shows that the transfer is accompanied by a relatively small change in the free energy, in agreement with experiments. A comparison of the potential of mean force with a continuum electrostatic model shows reasonable agreement. The mechanism of ion transfer across the interface under conditions of an external electric field is investigated by nonequilibrium molecular dynamics calculations. Despite the fact that this process has only a small free energy driving force, several of the structural and dynamical characteristics of the system during the transfer are similar to those observed in the study of the transfer of small ions with a large free energy of transfer.

I. Introduction

Ion transfer across the interface between two immiscible electrolyte solutions is a fundamental process of importance to diverse fields such as pharmacology,¹ electrochemistry,² analytical chemistry, and catalysis.³ Despite a century of experimental and theoretical studies of this process,⁴ several important questions remain open. This process can be viewed as a simple diffusion of an ion in an inhomogeneous media or as a chemical reaction involving a transition between two different solvation states. Despite the fact that in principle these are simple models, there is no quantitative theory that will allow one to predict the rate of ion transfer between the two liquids. For example, although the diffusion constant of ions in bulk liquids is simply related to the size of the ion,⁵ no such simple relation exists for the rate of transfer of the ion across an interface such as the one between water and nitrobenzene.⁶ Treating the ion transfer as an activated process such as a chemical reaction^{7–9} is also problematic. Although the transition state may be taken to be the ion with a mixed solvation shell, this does not provide sufficient information to characterize this state quantitatively. In addition, this description ignores the fact that the interface location, and more generally the interface structure, probably depends on the location of the ions. Evidence for this comes from molecular dynamics simulations.¹⁰

There are experimental and theoretical reasons for the fact that neither a quantitative theory nor a satisfactory mechanism of ion transfer has been proposed. The liquid/liquid interface is a buried interface whose size is much smaller than the size of the two bulk regions. Any information about a process which occurs at the interface must be disentangled from that coming from the bulk regions. This presents several experimental difficulties: For example, high bulk solution electrical resistance can mask the true kinetic resistance due to the ion transfer in measurements that are based on galvanostatic or potentiostatic methods. Other artifacts and difficulties are discussed extensively in the literature.^{6,11} As a result, values of the rate of ion transfer seem to depend on the technique used to measure them. However, this situation has been improving in recent years with advances in the design of microelectrodes¹² and electrochemical

cells⁶ and with the use of spectroscopic techniques to follow the ion transfer.^{13,14}

On the theoretical front, the main difficulties of developing a quantitative theory of ion transfer are the lack of knowledge about the structure of the interface and how this structure is affected by the presence of a finite concentration of ions. Indeed, even the structure of the neat interface of molecular liquids is an open problem in statistical mechanics.¹⁵ Additionally, developing theories of ion dynamics even in homogeneous liquids is an extremely challenging problem.¹⁶ It is not surprising therefore that molecular dynamics and Monte Carlo computer simulations which do not need to assume any underlying interface structure are very useful tools for elucidating the mechanism of ion transfer at the liquid/liquid interface.

Several molecular dynamics studies of ion (and neutral solute) transfer across the liquid/liquid interface have been reported in the past few years,^{10,17–22} focusing mainly on the calculation of the potential of mean force and less on the dynamics under realistic electrochemical conditions. We have previously studied the mechanism and dynamics of the transfer of small inorganic ions across the water/1,2-dichloroethane interface.^{10,18} This system is characterized by a large positive free energy of transfer of the ion from the aqueous to the organic phase. We concluded that the process involves a free energy barrier and that surface roughness (capillary “waves”) in the form of “fingers” is involved in the mechanism of the ion transfer. However, most experimental studies of ion transfer are done with larger ions, for which the free energy driving force is quite small. Many of these experiments are done at the water/nitrobenzene interface,^{23–25} whose properties are quite different from that of the water/1,2-dichloroethane interface. As a result, some of the conclusions of the study of the transfer of small ions across the water/1,2-dichloroethane interface may not be applicable to the transfer of larger ions across the water/nitrobenzene interface.

We have recently developed potential energy functions for the water/nitrobenzene system and studied the structure and dynamics of the interface by molecular dynamics computer simulations. We have found that, in general, despite the relatively large dielectric constant of the nitrobenzene ($\epsilon =$

TABLE 1: Lennard-Jones Parameters, and Partial Charges for Water, Nitrobenzene, and Tetramethylammonium

atom	σ (Å)	ϵ (kJ/mol)	Q (au)
C (bonded to NO ₂)	3.296	0.4184	0.150
C (ortho)	3.296	0.4184	-0.050
C (meta)	3.296	0.4184	-0.150
C (para)	3.296	0.4184	-0.050
N (NO ₂)	2.994	0.6276	-0.300
O (Nitro)	2.774	0.0335	0.150
H (ortho)	2.744	0.0335	0.100
H (meta)	2.744	0.0335	0.100
H (para)	2.744	0.0335	0.100
O (water)	3.165	0.6502	-0.820
H (water)	0.000	0.0000	0.410
CH ₃ (TMA)	3.960	0.6067	0.250
N (TMA)	3.800	0.2092	0.000

38.42), many of the properties of its neat interface with water are similar to those of other water/nonpolar organic liquids. In particular, on the nanometer-length scale, the interface should be thought of as a sharp and rough transition between the bulk of the two liquids. (Very recent X-ray reflectivity studies provide direct experimental evidence that immiscible water/organic liquid interfaces are indeed molecularly sharp.²⁶) In this paper, we present a study of the equilibrium and nonequilibrium transfer of a relatively large organic ion, tetramethylammonium ((CH₃)₄N⁺, TMA), across the water/nitrobenzene interface. The main result of the equilibrium calculations is the free energy profile for the ion transfer, which shows very little driving force (small free energy of transfer), in agreement with experiments. The nonequilibrium calculations involve driving the ion across the interface under the influence of an external electric field. The main result here is that the process of ion transfer involves a significant roughening of the interface and the existence of fingerlike structures despite the fact that the free energy of transfer is very small. However, one important difference between this system and the transfer of small ions is that in the latter case the ion keeps its hydration shell when it is transferred from the aqueous to the organic phase (at least on the simulation time scale of a few nanoseconds), whereas in the present system the ion is able to shed its solvation shell during the transfer process.

The rest of the paper is organized as follows: In section II, we describe the potential energy functions, the methodology for computing the potential of mean force, and the simulation parameters. In section III, we discuss the results, including the potential of mean force, equilibrium structure, and the dynamics of the ion transfer. We conclude in section IV with a summary of the main results.

II. Methods

1. Potential Energy Functions. We use the flexible simple point charge (SPC) model²⁷ for the water potential. In this model, each water molecule is represented by a Lennard-Jones sphere in which three point charges are embedded at the location of the oxygen and the hydrogens atoms. The Lennard-Jones parameters and the charges (given in Table 1) are selected to reproduce a number of the experimental properties of water. The relative location of the charges is allowed to change according to an intramolecular potential selected to reproduce the vibrational spectra of the gas phase water molecule.²⁸ This model of water has been used in a number of molecular dynamics simulations of bulk and interfacial water and of aqueous solutions.²⁹

The nitrobenzene intermolecular potential is an empirically derived, all-atoms model also represented by a Lennard-Jones

sphere (for each atom) in which a fixed point charge is embedded. The parameters for this potential have been developed earlier³⁰ and are given in Table 1. They were selected to reproduce the experimental dipole moment and the enthalpy of vaporization of the liquid (55 kJ/mol). They give rise to a diffusion constant ($D = 1.3 \times 10^{-9}$ m²/s) and a dielectric constant ($\epsilon = 42$) that are in reasonable agreement with experimental data.³¹ For the intramolecular potential we use harmonic bond-stretching and angle-bending, and standard torsional and improper torsional terms. The water–nitrobenzene interaction potential is also described using Coulomb plus Lennard-Jones terms with parameters that are determined using the combination rule for mixtures.³² The use of this approximation for the water–nitrobenzene interaction potential is justified by the fact that the computed³⁰ (28 erg/cm²) and experimental³³ (25 erg/cm²) surface tension for this system agree quite well. More details about the nitrobenzene and water–nitrobenzene potentials can be found elsewhere.³⁰

The tetramethylammonium ion is modeled as a five-center molecule (we use a united atom description of the CH₃ group). The intermolecular interactions are described using the Lennard-Jones plus Coulomb potential whose parameters were selected to reproduce the hydration enthalpy of this ion (value³⁴ = -455 kJ/mol). These parameters are also given in Table 1. The ion is fully flexible with an intramolecular potential that includes C–N harmonic stretching and C–N–C harmonic bending terms with the corresponding force constants and equilibrium bond-length and bond-angles taken from the Amber force field.³⁵

2. System Description and Other Simulation Details. The simulated system includes one TMA ion, 986 water molecules and 252 nitrobenzene molecules in a box of cross section 31.99 Å × 31.29 Å. The interface between the two liquids is perpendicular to the long axis of the box (which is taken to be the Z-direction) and on average is located at $Z = 0$. The total thickness of the slab along the Z-axis is approximately 80 Å. However, the length of the simulation box along the Z-axis is chosen to be long enough to avoid a second liquid/liquid interface. Thus, the geometry of the system is such that a single liquid/liquid interface is flanked between two bulk liquid regions, each of which is at equilibrium with its own vapor. Note that, although periodic boundary conditions in the Z-direction are enforced, during the simulation time scale of a few hundred picoseconds (see below), no mixing of the two vapor phases takes place. Other choices of simulation geometries and connections with statistical mechanical ensembles are discussed elsewhere.³⁶

The system is prepared by first equilibrating the neat interface and then introducing the ion in different locations. For the equilibrium mean force calculations, the ion is introduced into different locations and the data are collected after an equilibrium period long enough to give a stable value for the ion–liquids interaction energy (see below), typically a few tens of picoseconds. The nonequilibrium calculations are initiated by placing the ion in either of the two bulk phases. After a 50 ps equilibration, a fixed external electric field is applied in the Z-direction in order to drive the ion from one bulk phase to the other. Using the opposite field polarity allows us to investigate the reverse process. All the calculations are done at a temperature of $T = 300$ K using the velocity version of the Verlet algorithm³⁷ with a time step of 0.5 fs.

The proper handling of the long-range forces in simulations of polar systems is of particular concern in the study of charged solutes, and the Ewald summation method³⁷ has been used with some success in the study of ions in bulk liquids.^{38–40} It is not

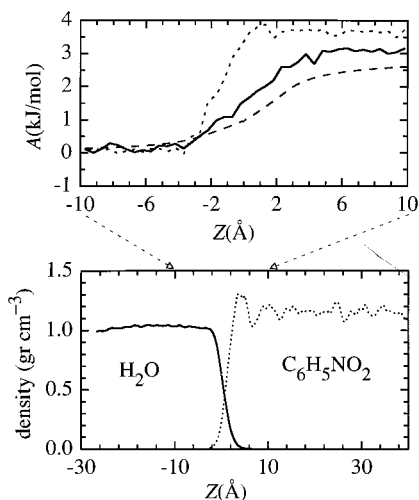


Figure 1. (Top panel) The potential of mean force for the transfer of TMA across the water-nitrobenzene interface: (solid line) calculated using the solute location distribution function; (dotted line) calculated using the integral of the average force on the ion; (dashed line) results of a continuum electrostatic model (eq 3). (Bottom panel) Density profiles of water and nitrobenzene showing the liquid/liquid interface region where the solute is located.

clear that the use of this method at liquid interfaces is justified because the artificial duplication of the inhomogeneous charge distribution may give rise to certain artifacts⁴¹ (such as interactions between the two surfaces generated by the periodic boundary conditions). Because we are interested here in the difference in the ion solvation free energy between two points that are close in space, we do not expect that long-range forces will significantly contribute to the system studied here. This was confirmed by estimating the contribution of the long-range forces by using the reaction field method.⁴²

3. Potential of Mean Force. We use two different techniques to compute the potential of mean force for the transfer of TMA across the water/nitrobenzene interface. Both techniques involve dividing the interval along the normal to the interface into overlapping slabs of thickness 3 Å and computing, as a function of the location z of the ion (along the interface normal), the average total z -component of force on the ion $\bar{F}_z(z)$ and the probability distribution of the ion location $P(z)$. The free energy profile is computed from the position probability distribution by combining together the free energy profiles calculated in the individual slabs

$$A_n(z) = -RT \ln P_n(z) \quad (1)$$

where $P_n(z)$ is the probability distribution in the n th slab. Alternatively, the free energy profile is the integral of the average force:

$$A(z_1) - A(z_2) = -\int_{z_1}^{z_2} \bar{F}_z(z) dz \quad (2)$$

These methods have been used to compute the free energy profile for neutral solutes and ions in a large number of interfacial systems. More details and an extensive list of references can be found in several recent review articles.^{29,36,43}

III. Results and Discussion

1. Potential of Mean Force and Equilibrium Structure.

The top panel of Figure 1 presents the results of the potential of mean force calculations using the two different techniques discussed above. Since our estimate for the statistical error in

these calculations is 1 kJ/mol in the interface region (the error is somewhat smaller in the regions outside the 12 Å interface region), we conclude that the two methods give consistent results. The potential of mean force is monotonically decreasing as the TMA is transferred from nitrobenzene to water. The free energy of transfer is 3 ± 1 kJ/mol, in good agreement with experiments. The bottom panel of Figure 1 shows the density profile of the two liquids in the system where the equilibrium calculations are done. Clearly, the change in the potential of mean force is mainly limited to the region where the density of the two liquids is varying. An examination of the structure of the solvation complex in this region shows that it is made up of a mixture of the two solvent molecules, as will be discussed below. This situation is somewhat different from the case of the transfer of small inorganic ions^{10,18} such as Na^+ and Cl^- . There, the potential of mean force varies by a larger amount and over a distance that extends beyond the region where the density of the liquid varies, reflecting the stronger and longer-range interactions between the water and the small ion. However, other characteristics of the transfer process discussed below show some similarity to those of the transfer of small ions.

It is interesting to compare the above results to a continuum electrostatic model of the free energy profile. This profile has been calculated by Ulstrup and Kharkats⁴⁴ for the transfer of a point charge q embedded in a spherical cavity of radius r . The interface is modeled as a mathematically sharp boundary separating two bulk media of dielectric constants ϵ_I and ϵ_{II} . The expression for the case where the center of the cavity is in medium I is given by

$$A(x \geq 1) = \frac{q^2}{2\epsilon_I r} \left[1 + \frac{f}{2x} + \frac{f^2}{4} \left(\frac{2}{1 - (2x)^2} + \frac{1}{2x} \ln \frac{2x + 1}{2x - 1} \right) \right]$$

$$A(0 \leq x \leq 1) = \frac{q^2}{4\epsilon_I r} \left[1 + x + (2 - x)f + \frac{f^2}{2} \left(\frac{(1 + x)(1 - 2x)}{1 + 2x} + \frac{1}{2x} \ln(1 + 2x) \right) \right] + \frac{q^2}{4\epsilon_{II} r} \left(\frac{2\epsilon_{II}}{\epsilon_I + \epsilon_{II}} \right)^2 (1 - x) \quad (3)$$

where $x = h/r$, h is the distance from the interface, and $f = (\epsilon_I - \epsilon_{II})/(\epsilon_I + \epsilon_{II})$. A similar expression is obtained when the ion is in the second medium by interchanging ϵ_I and ϵ_{II} . The profile calculated using this formula and the dielectric constants of the two liquids $\epsilon_I = 80$ (water) and $\epsilon_{II} = 42$ (nitrobenzene) is given as a dashed line in the top panel of Figure 1. The agreement is quite reasonable. In particular, the free energy of transfer compares favorably with experiments and with the MD results, and is given by

$$\Delta A_{\text{water} \rightarrow \text{nitrobenzene}} = \frac{q^2}{2r} \left(\frac{1}{\epsilon_{II}} - \frac{1}{\epsilon_I} \right) = 2.9 \text{ kJ/mol}$$

It is interesting to note that, in general, continuum electrostatic calculations of interfacial free energy are not found to be in quantitative agreement with simulations.³⁶ In particular, the potential of mean force for small ions across the water-1,2-dichloroethane interface¹⁰ and at the water liquid/vapor interface^{45,46} is in poor agreement with simulations. While the whole question of testing continuum models at interfaces is very much open, one should point out two major differences between the current system and those mentioned above. First, the TMA ion is much bigger and, thus, continuum solvent models should in general work better.⁴⁷ Second, the dielectric constants of water

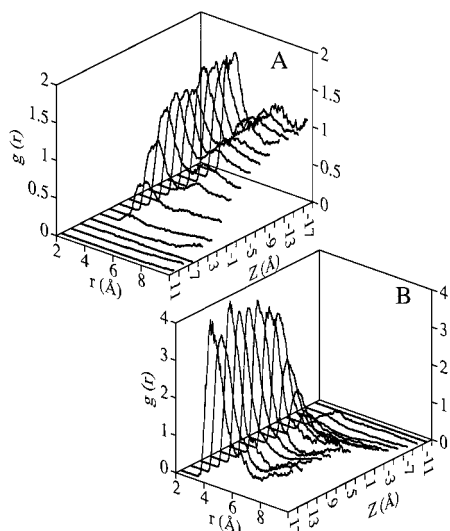


Figure 2. TMA–solvent radial distribution functions vs the location of the TMA along the interface normal: (A) nitrogen–TMA/oxygen water correlation functions; (B) nitrogen–TMA/oxygen nitrobenzene correlation functions.

and nitrobenzene are much closer to each other than those of water and the second phase in the water/vapor and water/1,2-dichloroethane systems. As a result, the image effects at the sharp boundary in the continuum model are less pronounced in the current system. These image effects are known to overestimate the energetics at short distances from the interface.⁴⁸

The equilibrium calculations that provide the data for the potential of mean force calculations enable us to study the structure of the TMA solvation complex. One way to examine the structure of this complex is to calculate the TMA–solvent atomic pair correlation functions $\rho_{\alpha\beta}(r, z_\alpha, z_\beta)$, which give the probability of finding the atom β located at a distance z_β along the interface normal and at a distance r from a solute atom located a distance z_α along the interface normal. Because this four-dimensional object is too detailed to display (or calculate!), we typically show the results averaged over the location z_β of the solvent atom, with a rather coarse binning of the location z_α . This provides a “bulklike” radial distribution function $g_{\alpha\beta}(r; z_\alpha)$ for the ions in different slabs relative to the interface. Figure 2 shows the radial distribution for the nitrogen of the TMA cation ($\alpha = \text{N}$) and either the oxygen of water ($\beta = \text{O}(\text{H}_2\text{O})$, panel A) or the oxygen of nitrobenzene ($\beta = \text{O}(\text{PhNO}_2)$, panel B). Other atoms of the nitrobenzene can be used with results that provide similar insight to what is discussed below. We choose to focus on the oxygen of the nitrobenzene because it provides the most detailed structure. Note that in bulk nitrobenzene, the oxygen of the solvent points toward the TMA cation.

The most significant feature of the data in Figure 2 is that the change in the equilibrium solvation structure is quite abrupt and limited to a region a few angstroms wide. For example, the water–TMA $g_{\alpha\beta}(r; z_\alpha)$ is almost constant up to $z_\alpha < -5$ (recall that the water slab is in the region $z < 0$), the main peak is down to 50% of the bulk value near the Gibbs surface ($z \approx 0$), and it is virtually zero for $z_\alpha > 5$. There is a corresponding parallel increase in the nitrobenzene–TMA correlation over a similar length scale. This is consistent with a gradual exchange of the TMA solvation shell over a distance of 1 nm. Of course this change in structure is mirrored in other properties such as the ion–solvent interaction energy. This will be discussed below when we compare the equilibrium situation with the nonequilibrium results.

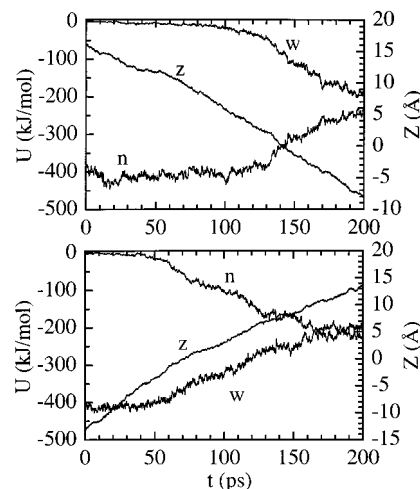


Figure 3. Dynamics of TMA ion transfer from nitrobenzene to water (top panel) and from water to nitrobenzene (bottom panel). In each panel the location of the ion along the interface normal (Z) is labeled “ z ” and is shown on the right axis. The TMA–solvent interaction energies are labeled “ w ” and “ n ” for the interaction with water and nitrobenzene, respectively. (left axis)

2. Nonequilibrium Ion Transfer Calculations. Typical interfacial ion transfer experiments, such as cyclic voltammetry, involve the measurement of the steady-state current of ions produced when an external electric field is applied across the liquid/liquid interface. The magnitude of the potential difference used in these experiments is on the order of a few volts. Since the potential change is mainly limited to the polarized region of the system, which is the interface region, the resulting electric field strength is on the order of 0.01–0.1 V/Å. Thus, an important part of the study of ion transfer mechanism and dynamics by molecular dynamics simulations must involve examining the transfer under these conditions.

In reality, the potential drop across the interface is established by a nonequilibrium ionic distribution in the double layer. Since a molecular dynamics study of a finite concentration of ions in a realistic model of molecular liquids at interfaces is not yet feasible, our approach to the inclusion of the external field of strength E_z is to add a constant force of magnitude qE_z along the direction normal to the interface on each atom of charge q . The calculations involve starting from a single ion in the bulk phase far enough from the interface (15 Å) that no appreciable interaction with the second phase exists. The external field polarity is selected so that the positively charged TMA ion moves toward the other phase. The trajectory is stopped when the ion reaches the bulk of the other phase (about 200 ps). This is repeated 20 times, starting from an independent initial position. The calculations are done for both the water → nitrobenzene and the nitrobenzene → water transfer. The strength of the electric field is 0.05 V/Å in all of the calculations reported below.

The results of all of the above calculations are summarized in Figure 3, where the average interaction energy of TMA with each liquid is shown as a function of time together with the average location of the ion. We show the averages rather than the distributions because the spread in the results is not very big, and the distributions are too noisy to be useful other than to show the general trend.

We first consider the rate of the ion transfer across the interface. By this we simply mean the average drift speed of the ion, which can be calculated from the slope of the average location of the ion as a function of time. From the overall

distance traveled in the 200 ps time interval we determine that $\bar{v}_{\text{nb}\rightarrow\text{w}} \approx [16.0 - (-8.0)] \text{ \AA}/200 \text{ ps} = 0.12 \text{ \AA}/\text{ps}$ (top panel) and $\bar{v}_{\text{w}\rightarrow\text{nb}} \approx [13.5 - (-13.0)] \text{ \AA}/200 \text{ ps} = 0.13 \text{ \AA}/\text{ps}$ (bottom panel), so that the transfer rate is almost the same for the two directions, and there is no significant slowing down as the ion crosses the interface relative to the motion in the bulk phases. A closer examination of the curves shows that when the ion starts in the organic phase (top panel) its average drift speed is $\bar{v}_{\text{nb}} \approx 0.20 \text{ \AA}/\text{ps}$, and its final value when it is in the water phase is $\bar{v}_{\text{w}} \approx 0.14 \text{ \AA}/\text{ps}$. Similar results are obtained from the bottom panel, where the ion starts at a higher speed $\bar{v}_{\text{w}} \approx 0.19 \text{ \AA}/\text{ps}$ when it is in the water phase and slows down by almost a factor of 2 when it is in the organic phase. These numbers are in complete agreement with a simple continuum model of ion mobility, taking into account the higher viscosity of nitrobenzene ($\eta = 1.795 \times 10^{-3} \text{ Pa}\cdot\text{s}$) than that of water ($\eta = 0.890 \times 10^{-3} \text{ Pa}\cdot\text{s}$, experimental values⁴⁹ at 298 K). We can estimate what the drift speed of the ion in the bulk of each liquid should be from the Stokes–Einstein law which is a reasonable approximation for an ion such as TMA. At steady state, the frictional force $f = 6\pi\eta r v$ on the ion of radius r moving at a speed v balances the electrical force qE_z , and so

$$v = qE_z / 6\pi\eta r \quad (4)$$

Substituting the above values of the viscosity, the radius of the ion $r = 2.74$ (half the CN bond length plus half the methyl Lennard-Jones parameter) and $E = 0.05 \text{ V/\AA}$ gives $\bar{v}_{\text{w}} \approx 0.17 \text{ \AA}/\text{ps}$ and $\bar{v}_{\text{nb}} \approx 0.09 \text{ \AA}/\text{ps}$, in excellent agreement with the molecular dynamics results.

Figure 3 also presents the average interaction energy of the ion with each of the two liquids during the transfer process. In both panels, the ion starts with the bulk value of the interaction energy with one of the liquids (which is near -400 kJ/mol in both cases) and with zero interaction energy with the other liquid. As the TMA ion moves from the water to the nitrobenzene (bottom panel), its interaction energy with the water molecules begins to decrease (absolute values) and, simultaneously, its interaction energy with the nitrobenzene begins to rise after about 50 ps. However, the lag time before there are changes in the interaction energies for the transfer from nitrobenzene to water (top panel) is twice as long. This simply reflects the slower motion of the ion in the organic phase, as elaborated above.

The most important feature of Figure 3 is the following: Although after 200 ps the ion is supposedly transferred from one phase to the other, the interaction energy with both liquids is still quite substantial—near 50% of the bulk value. Thus, for example, as the ion crosses from the organic to the water phase, the interaction with nitrobenzene weakens from near -400 kJ/mol to near -200 kJ/mol , while the interaction with water goes from 0 to -200 kJ/mol when the ion is at $Z = -13 \text{ \AA}$ (top panel). The bottom panel shows, however, that at this value of Z the ion is fully solvated by water. This extreme hysteresis suggests that as the ion crosses the interface from liquid A to B, a significant roughening of the interface occurs which enables the ion to keep strong contact with molecules of liquid A. This is confirmed by observation of actual simulation configurations. However, an examination of the trajectories shows that the ion does not keep a hydration shell as it transfers from water to nitrobenzene (or vice versa), but rather creates a fingerlike deformation in the interface. These interface deformations are found to be much more dramatic and longer-lived in the case of the transfer of small ions from the water to the organic (1,2-dichloroethane) phase,^{18,10} where the ions are found to keep part

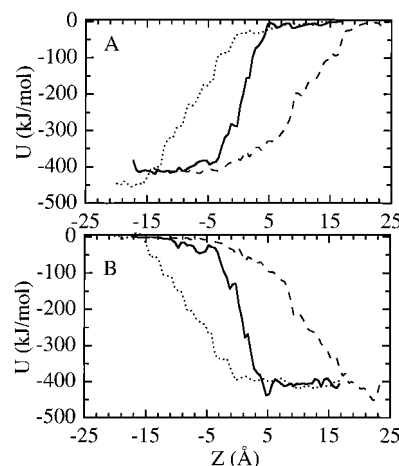


Figure 4. TMA–water (top panel) and TMA–nitrobenzene (bottom panel) interaction energy as a function of the location of TMA along the interface normal. In each panel the solid line is the result of the equilibrium calculations, the dotted line is obtained from the data during the transfer of TMA from nitrobenzene to water and the dashed line corresponds to the transfer of TMA from water to nitrobenzene.

of their hydration shell (on the simulation time scale), but it is interesting to note that these deformations appear here despite the fact that the ion does not keep a hydration shell. In fact, in one trajectory in which the TMA is transferred from water to nitrobenzene, the ion manages to get to $Z = 25 \text{ \AA}$ during the 200 ps time interval, and by then the interaction with water indeed decays to zero. Examination of the structure of the liquid interface shows that the interface roughness returns to “normal” values.

A simple way to demonstrate the fact that the ion does not keep a hydration shell is depicted in Figure 4, where the interaction energy of the TMA ion with water (top panel) and with nitrobenzene (bottom panel) are plotted as a function of the location of the ion for the equilibrium calculations (solid lines) and for the two nonequilibrium transfer calculations. The top panel shows that the interaction of TMA with water during the transfer of TMA into nitrobenzene (dashed line) varies more slowly (as a function of Z) than the equilibrium TMA–water interaction, and the same occurs during the reverse process (buildup of water–TMA interaction). The bottom panel shows the same effect for the TMA–nitrobenzene interactions. This corresponds to a delay in the switching of the solvation shell, which occurs farther along the “reaction coordinate” than the point indicated by the equilibrium calculations. For example, $Z \approx 0$ is the location where the TMA solvation shell is 50% water and 50% nitrobenzene from the equilibrium calculations. It is at 9 \AA when the ion leaves the water phase (that is 9 \AA inside the organic phase) and at -7 \AA when the ion leaves the organic phase.

Further support for the delay in the switching of the solvation shell structure is given in Figure 5, which shows the time-dependent TMA–water and TMA–nitrobenzene radial distribution functions. The top panels give the oxygen(water)–nitrogen(TMA) atomic distributions for the transfer of TMA from water to nitrobenzene (panel A) and for the transfer of TMA from nitrobenzene to water (panel B). Panel A shows that the main change in the radial distribution function is a linear decrease in the height of the first and second peaks of the distribution, without a change in the peaks’ locations. This is consistent with a gradual change in the hydration number. The much slower buildup of the distribution in the case of the transfer from nitrobenzene to water (panel B) is consistent with the above-mentioned delay in the switching of the solvation shell.

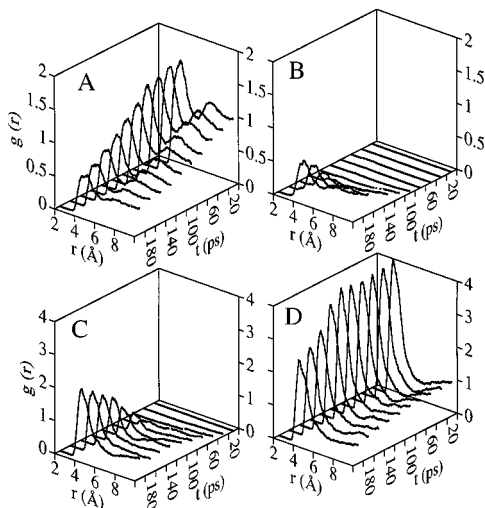


Figure 5. TMA–water (top two panels) and the TMA–nitrobenzene (bottom two panels) radial distribution functions vs time during the ion transfer process. In panels A and C we show the distribution during the transfer from water to nitrobenzene and in panels B and D during the reverse transfer.

The two bottom panels correspond to the oxygen(nitrobenzene)–nitrogen(TMA) atomic distributions for the transfer of TMA from water to nitrobenzene (panel C) and for the transfer of TMA from nitrobenzene to water (panel D). Similar to the water–TMA distributions, the buildup of the distribution as the TMA begins to interact with the nitrobenzene is linear in time with no change other than the increase in the height. On the other hand, the diminishing of the TMA–nitrobenzene distribution as the TMA is transferred to water (panel D) is qualitatively different from the water–TMA distributions (compares panel A and D). There is a long period where the distributions are almost unchanged, and only after about 100 ps can a decrease be seen. This is consistent with the results shown in panel B, which shows no buildup of the TMA–water distributions until after 100 ps. These results reflect the slower drift of the TMA in the organic phase, as was mentioned earlier in the discussion of Figure 3.

IV. Conclusions

The transfer of tetramethylammonium across the water/nitrobenzene interface involves only a small change in the solvation free energy, compared with a much larger free energy of transfer which accompanies the transfer of small inorganic ions (such as Na⁺). Unlike the transfer of small inorganic ions, TMA does not keep a hydration shell when going into the organic phase, in agreement with experiments. This is most clearly shown in Figure 4 (top panel), where the water–ion interaction is zero for $Z > 15 \text{ \AA}$ in the equilibrium calculations and for $Z > 25 \text{ \AA}$ in the nonequilibrium case. This delay in the “shedding off” of the hydration shell during the nonequilibrium transfer is accompanied by a significant increase in the surface roughness in the form of “fingering”. It is similar to (but less pronounced than) the case of the transfer of small ions. Continuum models description of both the equilibrium and the dynamics of this transfer seem to be reasonable: The dynamics of the ion transfer under the influence of an electric field obey the simple Stokes relation between the drift velocity and the electric field strength, and the potential of mean force is in good agreement with continuum electrostatics.

Acknowledgment. This work has been supported by the National Science Foundation grant no. CHE-9628072.

References and Notes

- (1) Arai, K.; Ohsawa, M.; Kusu, F.; Takamura, K. *Bioelectrochem. Bioenerg.* **1993**, *31*, 65.
- (2) Bard, A. J.; Faulkner, L. R. *Electrochemical methods: fundamentals and applications*; Wiley: New York, 1980.
- (3) Starks, C. M.; Liotta, C. L.; Halpern, M. *Phase Transfer Catalysis*; Chapman & Hall: New York, 1994.
- (4) Vanysek, P. *Electrochim. Acta* **1995**, *40*, 2841.
- (5) Impey, R. W.; Madden, P. A.; McDonald, I. R. *J. Phys. Chem.* **1983**, *87*, 5071.
- (6) Samec, Z. In *Liquid–Liquid Interfaces*; Volkov, A. G., Deamer, D. W., Eds.; CRC Press: Boca Raton, FL, 1996; p 155.
- (7) Gurevich, Y. Y.; Kharkats, Y. I. *J. Electroanal. Chem.* **1986**, *200*, 3.
- (8) Samec, Z.; Kharkats, Y. I.; Gurevich, Y. Y. *J. Electroanal. Chem.* **1986**, *204*, 257.
- (9) Girault, H. H.; Schiffrin, D. J. In *Electroanalytical Chemistry*; Bard, A. J., Ed.; Dekker: New York, 1989; p 1.
- (10) Schweighofer, K. J.; Benjamin, I. *J. Phys. Chem.* **1995**, *99*, 9974.
- (11) Girault, H. H. In *Modern Aspects of Electrochemistry*; Bockris, J. O. M., Conway, B. E., White, R. E., Eds.; Plenum Press: New York, 1993; Vol. 25; p 1.
- (12) Mirkin, M. V.; Fan, F.-R. F.; Bard, A. J. *Science* **1992**, *257*, 364.
- (13) Kakiuchi, T.; Takasu, Y. *J. Electroanal. Chem.* **1995**, *381*, 5.
- (14) Srivastava, A.; Eienthal, K. B. *Chem. Phys. Lett.* **1998**, *292*, 345.
- (15) *Fundamentals of Inhomogeneous Fluids*; Henderson, D., Ed.; Marcel Dekker: New York, 1992.
- (16) Wolynes, P. G. *Annu. Rev. Phys. Chem.* **1980**, *31*, 345.
- (17) Benjamin, I. *J. Chem. Phys.* **1992**, *96*, 577.
- (18) Benjamin, I. *Science* **1993**, *261*, 1558.
- (19) Hayoun, M.; Meyer, M.; Turq, P. *J. Phys. Chem.* **1994**, *98*, 6626.
- (20) Pohorille, A.; Wilson, M. A. *J. Chem. Phys.* **1996**, *104*, 3760.
- (21) Lauterbach, M.; Engler, E.; Muzet, N.; Troxler, L.; Wipff, G. *J. Phys. Chem. B* **1998**, *102*, 245.
- (22) Dang, L. X. Preprint, 1999.
- (23) Gavach, C.; D'Epenoux, B. *J. Electroanal. Chem.* **1974**, *55*, 59.
- (24) Kakiuchi, T.; Senda, M. *Bull. Chem. Soc. Jpn.* **1983**, *56*, 1753.
- (25) Kakiuchi, T.; Teranishi, Y. *J. Electroanal. Chem.* **1995**, *396*, 401.
- (26) Mitrinovic, D. M.; Zhang, Z.; Williams, S. M.; Huang, Z.; Schlossman, M. L. *J. Phys. Chem. B* **1999**, *103*, 1779.
- (27) Berendsen, H. J. C.; Postma, J. P. M.; Gunsteren, W. F. V.; Hermans, J. In *Intermolecular Forces*; Pullman, B., Ed.; D. Reidel: Dordrecht, 1981; p 331.
- (28) Kuchitsu, K.; Morino, Y. *Bull. Chem. Soc. Jpn.* **1965**, *38*, 814.
- (29) Benjamin, I. *Chem. Rev.* **1996**, *96*, 1449.
- (30) Michael, D.; Benjamin, I. *J. Electroanal. Chem.* **1998**, *450*, 335.
- (31) Lide, D. R. *Handbook of Chemistry and Physics*, 71st ed.; CRC Press: Boca Raton, FL, 1990.
- (32) Hansen, J.-P.; McDonald, I. R. *Theory of Simple Liquids*, 2nd ed.; Academic: London, 1986.
- (33) Adamson, A. W. *Physical Chemistry of Surfaces*, 5th ed.; Wiley: New York, 1990; p 111.
- (34) Maeda, M.; Ohtaki, H. *Bull. Chem. Soc. Jpn.* **1975**, *48*, 3755.
- (35) Weiner, S. J.; Kollman, P. A.; Nguyen, D. T.; Case, D. A. *J. Comput. Chem.* **1986**, *7*, 230.
- (36) Benjamin, I. In *Modern Methods for Multidimensional Dynamics Computations in Chemistry*; Thompson, D. L., Ed.; World Scientific: Singapore, 1998; p 101.
- (37) Allen, M. P.; Tildesley, D. J. *Computer Simulation of Liquids*; Clarendon: Oxford, UK, 1987.
- (38) Bader, J. S.; Chandler, D. *J. Phys. Chem.* **1992**, *96*, 6423.
- (39) Friedman, R. A.; Mezei, M. *J. Chem. Phys.* **1995**, *102*, 419.
- (40) Gunsteren, W. F. v.; Mark, A. E. *J. Chem. Phys.* **1998**, *108*, 6109.
- (41) Alejandre, J.; Tildesley, D. J.; Chapala, G. A. *J. Chem. Phys.* **1995**, *102*, 4574.
- (42) Barker, J. A. In *The problem of long-range forces in the computer simulation of condensed matter*; Ceperley, D., Ed.; NRCC Workshop Proceedings; 1980; Vol. 9, p 45.
- (43) Benjamin, I. *Annu. Rev. Phys. Chem.* **1997**, *48*, 401.
- (44) Ulstrup, J.; Kharkats, Y. I. *Elektrokhimiya* **1993**, *29*, 299.
- (45) Wilson, M. A.; Pohorille, A.; Pratt, L. R. *Chem. Phys.* **1989**, *129*, 209.
- (46) Benjamin, I. *J. Chem. Phys.* **1991**, *95*, 3698.
- (47) Frohlich, H. *Theory of dielectrics*; Clarendon: Oxford, UK, 1958.
- (48) Kharkats, Y. I.; Ulstrup, J. *Chem. Phys.* **1990**, *141*, 117.
- (49) Marcus, Y. *Ion Solvation*; Wiley: New York, 1985.